

## Blue phase liquid crystals stabilized by linear photo-polymerization

Daming Xu,<sup>1</sup> Jiamin Yuan,<sup>1</sup> Martin Schadt,<sup>2</sup> and Shin-Tson Wu<sup>1,a)</sup>

<sup>1</sup>CREOL, The College of Optics and Photonics, University of Central Florida, Orlando, Florida 32816, USA

<sup>2</sup>MS High-Tech Consulting, Liestalerstrasse 77, 4411 Seltisberg, Switzerland

(Received 31 July 2014; accepted 24 August 2014; published online 29 August 2014)

Stabilizing a photopolymer-embedded blue phase liquid crystal precursor with linearly polarized UV light is investigated experimentally. When the UV polarization axis is perpendicular to the stripe electrodes of an in-plane-switching cell, anisotropic polymer networks are formed through the linear photo-polymerization process and the electrostriction effect is suppressed. As a result, the measured hysteresis is dramatically reduced from 6.95% to 0.36% and the response time shortened by  $\sim 2\times$  compared to unpolarized UV exposure. To induce larger anisotropy in polymer networks for mitigating the electrostriction effect, high-intensity linearly polarized UV exposure is preferred. © 2014 AIP Publishing LLC. [<http://dx.doi.org/10.1063/1.4894727>]

Polymer-stabilized blue phase liquid crystals (PS-BPLCs)<sup>1,2</sup> are promising candidates for next-generation displays<sup>3,4</sup> and photonic devices.<sup>5–7</sup> Compared to commonly employed nematic liquid crystals,<sup>8,9</sup> PS-BPLCs exhibit several attractive features such as submillisecond response times,<sup>10,11</sup> no need for surface alignment, and an optically isotropic dark state. After one decade of extensive efforts, major technical barriers of PS-BPLCs have gradually been overcome. Their operation voltage has been reduced from 50 V to below 10 V by employing large Kerr constant BPLC materials<sup>12–14</sup> and implementing device structures with enhanced penetrating fields.<sup>15–17</sup> High transmittance ( $>80\%$ ) can be achieved by optimizing the refraction effect of the non-uniform fringing electric fields.<sup>18</sup> Moreover, a contrast ratio over 3000:1 has been demonstrated by compensating the polarization rotation effect of PS-BPLC cells.<sup>19</sup>

In terms of device configuration, both in-plane-switching (IPS)<sup>16,20</sup> and vertical field switching<sup>21–23</sup> modes have been developed. Between these two, IPS is more commonly employed because of its simpler backlight system. However, for IPS cells, hysteresis and prolonged response times, especially in the high field region, remain technical challenges.<sup>24,25</sup> From previous studies, three electric field-induced effects occur in PS-BPLCs with increasing electric fields: local LC director reorientation governed by Kerr effect,<sup>26</sup> lattice distortion induced by electrostriction,<sup>27,28</sup> and finally transition into a LC phase with lower symmetry.<sup>29</sup> The response time of the Kerr effect is usually in the submillisecond range,<sup>11</sup> but the latter two processes take several milliseconds or even longer.<sup>29</sup> When the electric field is below a critical field ( $E < E_c$ ), Kerr effect dominates, which means that the response time is fast and the hysteresis is negligible. However, for  $E > E_c$ , electrostriction gradually develops,<sup>30</sup> causing both response time and hysteresis to increase dramatically. Hysteresis affects the accuracy of grayscale control and should be suppressed. Moreover, if the response time of BPLCs increases into the millisecond range, then a major advantage over nematic LCs disappears. Therefore, there is an urgent need for suppressing the electrostriction

effect in order to achieve submillisecond response time and hysteresis-free BPLC devices.

In this letter, we propose an approach for suppressing the electrostriction effect by polymerizing photopolymers with linearly polarized UV light instead of conventional unpolarized UV. We found that linear photo-polymerization (LPP)<sup>30</sup> can induce an anisotropic polymer network in the bulk of BPLCs, generating anisotropic electrostriction with respect to the direction of applied electric fields. By setting the polarization direction of the crosslinking UV light perpendicular to the stripe electrodes of an IPS cell, the electrostriction effect is dramatically suppressed. As a result, the hysteresis diminishes from 6.95% to 0.36% and the response time is improved by  $\sim 2\times$ , as compared to unpolarized UV curing.

To control the PS-BPLC lattice dimension, two types of monomers are commonly used: a di-functional (e.g., RM257) monomer and mono-functional (e.g., C12A; dodecyl acrylate) or tri-functional monomer (e.g., TMPTA; 1,1,1-Trimethylolpropane Triacrylate). Their chemical structures have been reported previously.<sup>3,31</sup> In the past, the polymerization process of pre-polymers in PS-BPLC was commonly conducted by using unpolarized UV light. However, the photo-crosslinking mechanism of pre-polymers is polarization-dependent.<sup>32,33</sup> For example, the crosslinking probability of a dichroic acrylate moiety is greater when exposed to UV light whose polarization axis is parallel to the double bonds instead of perpendicular. Therefore, by crosslinking double bonds with a linearly polarized UV light, anisotropic polymer networks can be formed. By controlling the UV polarization axis with respect to the direction of the stripe electrodes of an IPS-BPLC cell, the formed anisotropic polymer network could result in anisotropic electrostriction correspondingly.

In our experiments, we employed a large  $\Delta\epsilon$  nematic LC host JC-BP07N (JNC, Japan) whose physical properties are:  $\Delta n = 0.162$  at  $\lambda = 633$  nm,  $\Delta\epsilon = 302$  at 100 Hz and 22 °C, and  $T_c = 87$  °C. The BPLC precursor consists of 86.53 wt. % JC-BP07N, 2.82 wt. % chiral dopant R5011 (HCCH), 6.31 wt. % RM257 (Merck), 4.02 wt. % C12A (Sigma Aldrich), and 0.32 wt. % photoinitiator. The BPLC precursor was heated to an isotropic phase and then filled into IPS cells (cell gap  $d \sim 7.3$   $\mu\text{m}$ ). The cells comprise interdigitated pixel

<sup>a)</sup>Electronic mail: swu@ucf.edu

electrodes on the bottom substrates (electrode width  $w = 8 \mu\text{m}$  and spacing  $l = 12 \mu\text{m}$ ) without polyimide alignment layer. Next, the cells were placed on a Linkam temperature controllable stage, cooled to a temperature close to the chiral nematic and blue phase transition temperature, and then illuminated with UV light for 15 min ( $\lambda \sim 365 \text{ nm}$ , intensity of  $8 \text{ mW/cm}^2$ ).

To investigate the effect of UV polarization on the electro-optic properties of PS-BPLCs, we first prepared three IPS samples exposed under different UV polarization conditions: Sample 1: UV polarization direction parallel to the stripe electrodes, Sample 2: UV polarization perpendicular to the stripe electrodes, and Sample 3: unpolarized UV light. To rule out possible disturbing influences due to temperature cooling rate and curing temperature,<sup>34,35</sup> we kept these two parameters identical for all three samples. A linear UV polarizer was placed between UV light source and BPLC cell in all polarized-exposure experiments. After UV exposure, the nanostructured BPLC composite was self-assembled and the LPP-induced anisotropic polymer networks of samples 1 and 2 are sketched in Figs. 1(a) and 1(b), respectively. In the next step, the IPS cell was sandwiched between two crossed polarizers and a He-Ne laser was used as a probing beam ( $\lambda = 633 \text{ nm}$ ). The voltage-dependent transmitted light was focused by a lens so that different diffraction orders<sup>7</sup> could be collected by the detector.

To evaluate the degree of electrostriction, we measured the hysteresis of each sample by increasing the voltage to their individual peak transmittance and then sweeping it back to zero. Figure 2 depicts the measured hysteresis loop of samples 1–3. Their operation voltage, hysteresis, and response time are listed in Table I. From the table, we find that sample 2 (UV polarization is perpendicular to the stripe IPS electrodes) exhibits a much smaller hysteresis than sample 3 (unpolarized light).

The physical mechanism is explained as follows. As illustrated in Fig. 1(b), in the BPLC precursor containing

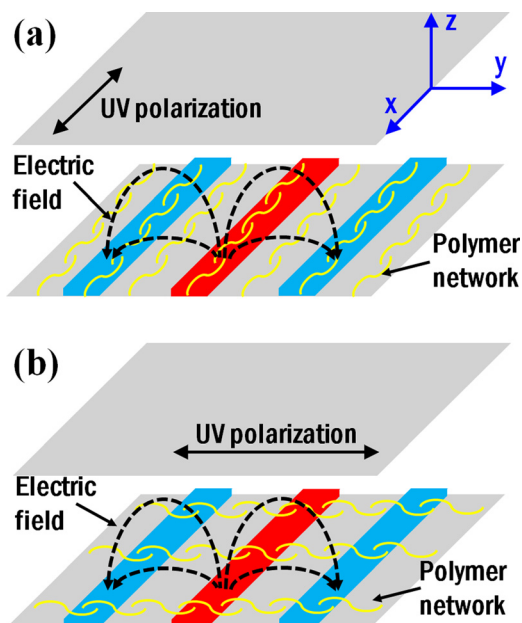


FIG. 1. LPP-induced anisotropic polymer network in (a) sample 1 and (b) sample 2.

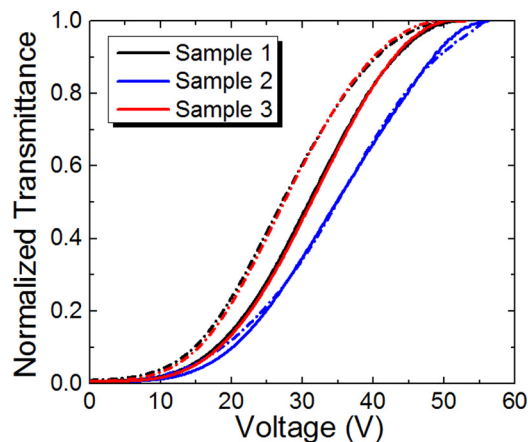


FIG. 2. Measured hysteresis loops of samples 1–3 (solid lines: forward driving, dashed lines: backward driving).

C12A and RM257 monomers, the directional LPP photoreaction is parallel to the polarization axis of the incident linearly polarized UV radiation. As a result, the polymer network is stronger along the UV polarization axis,<sup>32,36</sup> i.e., parallel to the direction of the applied electric field in sample 2. Therefore, the polymer network is more robust against electric field-induced deformation or distortion along the LPP direction, leading to a suppressed electrostriction effect and a reduced hysteresis as shown by sample 2. However, for UV polarization parallel to the stripe electrodes (sample 1), the polymer network forms mainly along the electrode direction and is therefore less robust along the direction of the applied electric field (cf., Fig. 1(a)). Consequently, the polymer network is more likely to be distorted or deformed by the applied electric field in the configuration of Fig. 1(a), resulting in severe electrostriction. This is indeed observed in sample 1, which exhibits the largest hysteresis (7.56%) as depicted in Fig. 2.

In some previous studies, the occurrence of electrostriction effect could be detected by measuring the shift of Bragg reflection wavelength.<sup>27,37</sup> These LC cells were with homogeneous alignment, in which the deformation of cubic lattice would shift the Bragg reflection wavelength. In contrast, our LC cells do not have any alignment layers, and the electric field is mainly in the horizontal plane. Therefore, the shift in Bragg reflection wavelength is very small and difficult to detect. Nevertheless, the ratio of electrostriction effect can still be distinguished from the dynamic response processes. According to the previous study, the suppressed electrostriction

TABLE I. Measured operation voltage, hysteresis, rise time, and decay time of samples 1–6.

	$V_{\text{on}}$ (V)	Hysteresis (%)	$\tau_{\text{rise}}$ ( $\mu\text{s}$ )	$\tau_{\text{decay}}$ (ms)
Sample 1	51.8	7.56	674.6	4.34
Sample 2	56.2	0.36	456.8	1.90
Sample 3	53.0	6.95	524.7	3.72
Sample 2a	57.4	0.33	437.4	1.97
Sample 2b	55.6	0.87	472.1	1.71
Sample 4	57.2	4.37	362.9	0.96
Sample 5	58.0	3.97	369.3	0.81
Sample 6	58.0	4.14	345.8	0.87

effect leads to smaller hysteresis and much faster response time.<sup>30</sup>

As listed in Table I, among samples 1–3, sample 2 exhibits the fastest rise and decay times, while sample 1 is the slowest. To explain the difference, we used our double relaxation model to describe the decay process.<sup>30</sup> This model properly reveals the contributions of Kerr effect and electrostriction effect on the electro-optic properties of a PS-BPLC device. In the following experiments, each cell was driven to its own peak transmittance after which the voltage was instantaneously removed. In order to compensate the polarization rotation effect originated from the BPLC layer, the analyzer was rotated by a small angle ( $\sim 2^\circ$ ) and the measured contrast ratio was over 2000:1.<sup>19</sup> The transient transmittance change was recorded by a digital oscilloscope. The measured change in transmittance  $T$  is related to the phase retardation  $\varphi$  by

$$T = \sin^2(\varphi/2). \quad (1)$$

The black solid line in Fig. 3 shows the measured transient phase retardation of sample 2 during the decay process. We then fit the experimental data with the following double relaxation equation:<sup>30</sup>

$$\varphi(t) = A_1 e^{-t/t_1} + A_2 e^{-t/t_2}, \quad (2)$$

where  $t_1$  and  $t_2$  are the average decay time constants and  $A_1$  and  $A_2$  are the phase retardations due to Kerr effect and electrostriction, respectively. The fitting curve (red solid line) in Fig. 3 shows that Eq. (2) describes the decay process of the phase retardation well. Table II lists the fitted time constants and the contribution of electrostriction effect, which are described by  $A_2/(A_1 + A_2)$  in our model.<sup>30</sup> All the values of  $t_1$  lie in the submillisecond range, while those of  $t_2$  are several milliseconds. This corresponds well with the fast Kerr effect and the slow electrostriction effect. Please note that sample 2 exhibits the fastest response time. This is due to the suppression of electrostriction by polarized crosslinking, which can be seen from the smallest  $A_2/(A_1 + A_2)$  ratio of sample 2. However, from Fig. 1, the non-planar electric field at the edges of planar stripe electrodes is still quite strong;<sup>38</sup> therefore the electrostriction effect is still not negligible (16.9%). Nevertheless, compared to sample 3, which is stabilized by

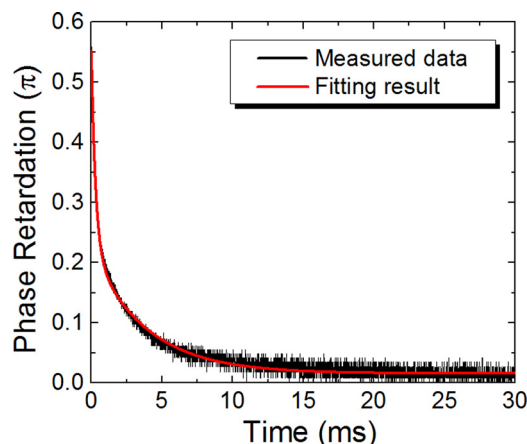


FIG. 3. Transient decay process of sample 2 at 56.2 V.

TABLE II. Fitted time constant  $t_1$  and  $t_2$  and contribution of electrostriction effect in samples 1–3.

	$T_1$ (ms)	$t_2$ (ms)	$A_2/(A_1 + A_2)$ (%)
Sample 1	0.51	6.47	43.8
Sample 2	0.27	3.78	16.9
Sample 3	0.39	5.98	38.7

unpolarized UV light, this ratio is more than  $2\times$  smaller. By using protruded electrodes instead of planar electrodes,<sup>38</sup> the on-state voltage would drop to below 10 V and the electrostriction effect should be completely suppressed. As a result, the response time should be in the submillisecond range over the entire driving voltage range.

More importantly, the results of our approach are quite reproducible. We prepared two more samples under the same conditions as sample 2, designated as samples 2a and 2b. Their operation voltage, hysteresis, and response time of these samples are also included in Table I. It clearly shows that the measured hysteresis of all these three samples is  $<1\%$ , which can be regarded as hysteresis-free. All the response times are also very close and faster than those of samples 1 and 3.

Meanwhile, the illumination intensity of polarized UV light affects the rate and the anisotropy of the crosslinking process. Thus, UV intensity also plays an important role in the LPP process. Using LPP-photoalignment (which employs polarized UV light to induce anisotropic LC-surface alignment)<sup>32</sup> as an analogy, the induced surface anchoring of LPP-photoalignment is related to the intensity of the activating UV light.<sup>39</sup> This trend also applies to polarized UV-polymerized PS-BPLC.

In addition to sample 2, we prepared for comparison two more samples using different UV exposure intensities. The UV dosage for all three samples was the same: 8 mW/cm<sup>2</sup> for 15 min, 4 mW/cm<sup>2</sup> for 30 min, and 2 mW/cm<sup>2</sup> for 60 min. The measured hysteresis loops of these three samples are plotted in Fig. 4, and the numerical values of their operation voltages, hysteresis, and response times are listed in Table III. With increasing UV exposure intensity, electrostriction is suppressed, resulting in faster response time and

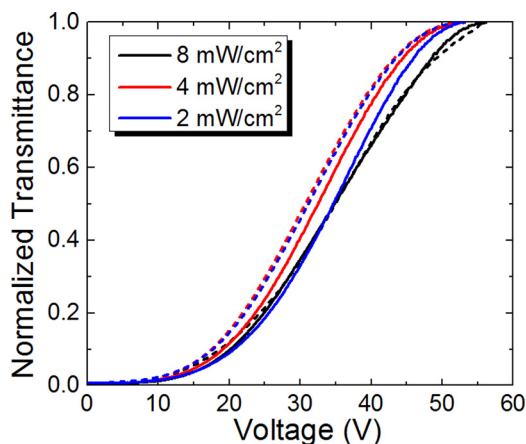


FIG. 4. Measured hysteresis loops of IPS cells under different UV illumination intensities (solid lines: forward driving, dashed lines: backward driving).



TABLE III. Measured operation voltage, hysteresis, and response times of IPS cells under different UV illumination intensities.

UV intensity (mW/cm <sup>2</sup> )	V <sub>on</sub> (V)	Hysteresis (%)	$\tau_{\text{rise}}$ ( $\mu$ s)	$\tau_{\text{decay}}$ (ms)
2	53.2	6.79	860.5	3.67
4	54.0	3.40	594.5	2.78
8	56.2	0.36	456.8	1.90

reduced hysteresis. This trend is similar to the LPP process of azo-type monomers, in which the diffusion rate of linearly polarized pre-polymers is proportional to the illumination power according to a diffusion model of photopolymers.<sup>39</sup> Hence, here we use this model as an analogy to explain the correlation of UV intensity and LPP-induced anisotropy in PS-BPLC. The higher diffusion rate under stronger UV illumination power is expected to result in a larger anisotropy of polymer networks. Consequently, a stronger polymer network forms along the electric field direction, thus suppressing electrostriction. In analogy, lower UV illumination power reduces the anisotropy of polymer networks. Hence, to induce a large anisotropy in the polymer networks of PS-BPLCs for minimizing electrostriction, strong linearly polarized UV light is preferred.

Besides the above RM257 and C12A monomer combination, we also investigated the effect of LPP on the electro-optic properties of PS-BPLCs by using another monomer combination, namely, the di-functional monomer RM257 and the tri-functional monomer TMPTA. The blue phase precursor consists of 86.90 wt. % JC-BP07N, 2.81 wt. % chiral dopant R5011, 5.98 wt. % RM257, 3.99 wt. % TMPTA, and 0.32 wt. % photoinitiator. Moreover, we also prepared three IPS samples under different UV curing conditions: Sample 4: UV polarization parallel to stripe electrodes; Sample 5: UV polarization perpendicular to stripe electrodes; and Sample 6: unpolarized UV light. All three samples were polymerized with the same UV dosage: 8 mW/cm<sup>2</sup> for 15 min. Figure 5 shows the measured hysteresis loops. The detailed operation voltage, hysteresis, and response time of these samples are also included in Table I. Compared to the combination of RM257 and C12A, the samples comprising RM257 and TMPTA do not exhibit large differences in terms of operation voltage, hysteresis, and response time under different UV polarization directions. This is because

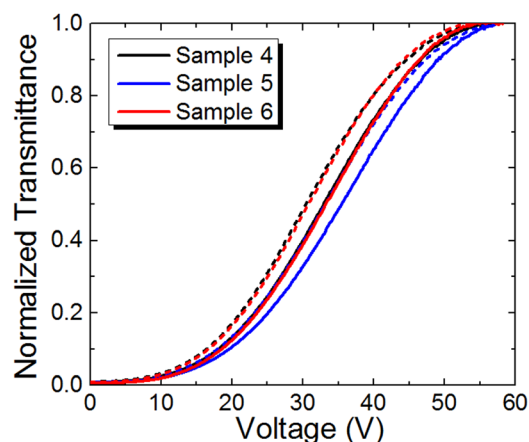


FIG. 5. Measured hysteresis loops of samples 4–6 (solid lines: forward driving, dashed lines: backward driving).

the tri-functional monomer TMPTA has three photocrosslinking double bonds along different directions, thus rendering their polymer networks more likely to be isotropic even under linearly polarized UV light.

In conclusion, we propose a method to suppress the electrostriction in PS-BPLCs via polymerizing photopolymers with linearly polarized UV light. By illuminating the mono-functional monomer C12A and the di-functional monomer RM257 with linearly polarized UV light, anisotropic polymer networks are formed, resulting in anisotropic electrostriction. Linear polarization of the cross-linking UV light perpendicular to the stripe electrodes strongly suppresses electrostriction. The resulting hysteresis is reduced from 6.95% to 0.36% and the response times improve by a factor of two. To induce a larger anisotropy in the polymer network which further reduces the electrostriction effect, a more powerful linearly polarized UV exposure is required.

The authors are indebted to Dr. Yasuhiro Haseba of JNC for providing the JC-BP07N sample, Fenglin Peng and Yuan Chen for technical assistance and useful discussion, and Industrial Technology Research Institute (ITRI, Taiwan) for the financial support.

- <sup>1</sup>H. Kikuchi, M. Yokota, Y. Hisakado, H. Yang, and T. Kajiyama, *Nat. Mater.* **1**, 64 (2002).
- <sup>2</sup>F. Peng, Y. Chen, J. Yuan, H. Chen, S. T. Wu, and Y. Haseba, *J. Mater. Chem. C* **2**, 3597 (2014).
- <sup>3</sup>J. Yan, L. Rao, M. Jiao, Y. Li, H. C. Cheng, and S. T. Wu, *J. Mater. Chem.* **21**, 7870 (2011).
- <sup>4</sup>Z. Luo, D. Xu, and S. T. Wu, *J. Disp. Technol.* **10**, 526 (2014).
- <sup>5</sup>W. Cao, A. Munoz, P. Palfy-Muhoray, and B. Taheri, *Nat. Mater.* **1**, 111 (2002).
- <sup>6</sup>Y. H. Lin, H. S. Chen, H. C. Lin, Y. S. Tsou, H. K. Hsu, and W. Y. Li, *Appl. Phys. Lett.* **96**, 113505 (2010).
- <sup>7</sup>J. Yan, Y. Li, and S. T. Wu, *Opt. Lett.* **36**, 1404 (2011).
- <sup>8</sup>D. K. Yang and S. T. Wu, *Fundamentals of Liquid Crystal Devices* (Wiley, New Jersey, 2006).
- <sup>9</sup>D. Xu, L. Rao, C. D. Tu, and S. T. Wu, *J. Disp. Technol.* **9**, 67 (2013).
- <sup>10</sup>K. M. Chen, S. Gauza, H. Q. Xianyu, and S. T. Wu, *J. Disp. Technol.* **6**, 49 (2010).
- <sup>11</sup>Y. Chen, J. Yan, J. Sun, S. T. Wu, X. Liang, S. H. Liu, P. J. Hsieh, K. L. Cheng, and J. W. Shiu, *Appl. Phys. Lett.* **99**, 201105 (2011).
- <sup>12</sup>M. Wittek, N. Tanaka, D. Wilkes, M. Bremer, D. Pauluth, J. Canisius, A. Yeh, R. Yan, K. Skjonnemand, and M. Klasen-Memmer, *SID Int. Symp. Dig. Tech. Pap.* **43**, 25 (2012).
- <sup>13</sup>Y. Chen, D. Xu, S. T. Wu, S. Yamamoto, and Y. Haseba, *Appl. Phys. Lett.* **102**, 141116 (2013).
- <sup>14</sup>Y. Haseba, S. Yamamoto, K. Sago, A. Takata, and H. Tobata, *SID Int. Symp. Dig. Tech. Pap.* **44**, 254 (2013).
- <sup>15</sup>M. Kim, M. S. Kim, B. G. Kang, M. K. Kim, S. Yoon, S. H. Lee, Z. Ge, L. Rao, S. Gauza, and S. T. Wu, *J. Phys. D: Appl. Phys.* **42**, 235502 (2009).
- <sup>16</sup>L. Rao, Z. Ge, S. T. Wu, and S. H. Lee, *Appl. Phys. Lett.* **95**, 231101 (2009).
- <sup>17</sup>L. Rao, H. C. Cheng, and S. T. Wu, *J. Disp. Technol.* **6**, 287 (2010).
- <sup>18</sup>D. Xu, Y. Chen, Y. Liu, and S. T. Wu, *Opt. Express* **21**, 24721 (2013).
- <sup>19</sup>Y. Liu, Y. F. Lan, H. Zhang, R. Zhu, D. Xu, C. Y. Tsai, J. K. Lu, N. Sugiura, Y. C. Lin, and S. T. Wu, *Appl. Phys. Lett.* **102**, 131102 (2013).
- <sup>20</sup>Z. Ge, S. Gauza, M. Jiao, H. Xianyu, and S. T. Wu, *Appl. Phys. Lett.* **94**, 101104 (2009).
- <sup>21</sup>H. C. Cheng, J. Yan, T. Ishinabe, N. Sugiura, C. Y. Liu, T. H. Huang, C. Y. Tsai, C. H. Lin, and S. T. Wu, *J. Disp. Technol.* **8**, 98 (2012).
- <sup>22</sup>H. C. Cheng, J. Yan, T. Ishinabe, and S. T. Wu, *Appl. Phys. Lett.* **98**, 261102 (2011).
- <sup>23</sup>J. Yan, D. Xu, H. C. Cheng, S. T. Wu, Y. F. Lan, and C. Y. Tsai, *Appl. Opt.* **52**, 8840 (2013).
- <sup>24</sup>K. M. Chen, S. Gauza, H. Xianyu, and S. T. Wu, *J. Disp. Technol.* **6**, 318 (2010).

- <sup>25</sup>Y. Liu, S. Xu, D. Xu, J. Yan, Y. Gao, and S. T. Wu, *Liq. Cryst.* **41**, 1339 (2014).
- <sup>26</sup>J. Yan, H. C. Cheng, S. Gauza, Y. Li, M. Jiao, L. Rao, and S. T. Wu, *Appl. Phys. Lett.* **96**, 071105 (2010).
- <sup>27</sup>G. Heppke, M. Krumrey, and F. Oestreicher, *Mol. Cryst. Liq. Cryst.* **99**, 99 (1983).
- <sup>28</sup>H. Choi, H. Higuchi, and H. Kikuchi, *Appl. Phys. Lett.* **98**, 131905 (2011).
- <sup>29</sup>H. S. Kitzerow, P. P. Crooker, S. L. Kwok, J. Xu, and G. Heppke, *Phys. Rev. A* **42**, 3442 (1990).
- <sup>30</sup>D. Xu, J. Yan, J. Yuan, F. Peng, Y. Chen, and S. T. Wu, *Appl. Phys. Lett.* **105**, 011119 (2014).
- <sup>31</sup>Y. Chen and S. T. Wu, *J. Appl. Polym. Sci.* **131**, 40556 (2014).
- <sup>32</sup>M. Schadt, K. Schmitt, V. Kozinkov, and V. Chigrinov, *Jpn. J. Appl. Phys., Part 1* **31**, 2155 (1992).
- <sup>33</sup>M. Schadt, H. Seiberle, and A. Schuster, *Nature* **381**, 212 (1996).
- <sup>34</sup>C. Y. Fan, H. C. Jau, T. H. Lin, F. C. Yu, T. H. Huang, C. Y. Liu, and N. Sugiura, *J. Disp. Technol.* **7**, 615 (2011).
- <sup>35</sup>S. B. Ni, J. L. Zhu, J. Tan, X. Y. Sun, E. W. Zhong, Y. J. Wang, C. P. Chen, Z. C. Ye, G. F. He, J. G. Lu, and Y. K. Su, *Opt. Mater. Express* **3**, 928 (2013).
- <sup>36</sup>M. Schadt, H. Seiberle, A. Schuster, and S. M. Kelly, *Jpn. J. Appl. Phys., Part 1* **34**, 3240 (1995).
- <sup>37</sup>S. Y. Lu and L. C. Chien, *Opt. Lett.* **35**, 562 (2010).
- <sup>38</sup>L. Rao, J. Yan, S. T. Wu, Y. C. Lai, Y. H. Chiu, H. Y. Chen, C. C. Liang, C. M. Wu, P. J. Hsieh, S. H. Liu, and K. L. Cheng, *J. Disp. Technol.* **7**, 627 (2011).
- <sup>39</sup>V. Chigrinov, S. Pikin, A. Verevochnikov, V. Kozenkov, M. Khazimullin, J. Ho, D. D. Huang, and H. S. Kwok, *Phys. Rev. E* **69**, 061713 (2004).